Proceedings of the
4th JSME-KSME Thermal Engineering Conference
October 1-6, 2000, Kobe, Japan

G109

THEORETICAL STUDY ON THE OPTIMIZATION OF FIN GEOMETRY FOR CONDENSATION OF R410A IN A HORIZONTAL MICROFIN TUBE

Huasheng WANG and Hiroshi HONDA

Institute of Advanced Material Study, Kyushu University, Kasuga, Fukuoka 816-8580, Japan

ABSTRACT A theoretical study was made to optimize the fin geometry of a helically-grooved, horizontal microfin tube for condensation of R410A. Numerical calculations of overall heat transfer from the vapor flowing inside the microfin tube to the surrounding air were conducted for typical operating conditions of an air-cooled condenser. The previously proposed stratified flow model was applied to the condensation heat transfer inside the tube. The numerical results showed that the effects of the length of flat portion at the fin tip, radius of round corner at the fin tip and the fin half tip angle are small and the effects of the fin height, fin number and helix angle of groove are of significance.

Keywords: Condensation, Refrigerant R410A, Microfin Tube, Fin Geometry Effect, Numerical Analysis

INDRODUCTION

Helically grooved, horizontal microfin tubes have been commonly used in air conditioners due to their high heat transfer performance. Many experimental studies reporting on the effects of fin geometry, tube diameter, refrigerant, oil etc. on the condensation heat transfer and pressure drop have been published. Webb [1] and Newell and Shah [2] have given comprehensive reviews of relevant literature. Cavallini et al. [3] and Shikazono et al. [4] have developed empirical equations of the circumferential average heat transfer coefficient. Yang and Webb [5] and Nozu and Honda [6], respectively, proposed a semi-empirical model and an annular flow model of condensation in microfin tubes which considered the combined effects of vapor shear and surface tension forces. Honda et al. [7] proposed a stratified flow model which considered the combined effects of surface tension and gravity. The height of stratified condensate was determined by a modified Taitel and Dukler [8] model which assumed a flat vapor-liquid interface. They showed that previous experimental data for four refrigerants and three tubes with relatively large fin height (h > 0.16mm) and relatively large diameters at fin root ($d = 8.5 \sim 8.8$mm) could be predicted within ±20% by the higher of the two theoretical predictions. Wang and Honda [9] extended the previously proposed model to include the effect of curved vapor-liquid interface that was caused by the surface tension. This model gave a better agreement (-7~22% as compared 1~31% of the flat interface model) with experimental data for R22 condensing in a tube with $d = 6.5$ mm.

The objective of the present work is to apply the previously proposed stratified flow model [7, 9] to an air-cooled condenser and study the effect of fin geometry on condensation of R410A. Assuming typical operating conditions of an air-cooled condenser, numerical calculations are conducted with systematically changed values of the fin number, fin height, helix angle of groove, fin half-tip angle, etc.

ANALYSIS

Physical Model

We consider a horizontal air-cooled condenser as shown in Fig.1 in which R410A is condensed. The refrigerant is assumed to be dry saturated ($\chi = 1$) at the condenser inlet and $\chi = 0$ at the condenser outlet. The refrigerant mass velocity G is assumed to be 50, 100 and 300 kg/m^{2}s, and

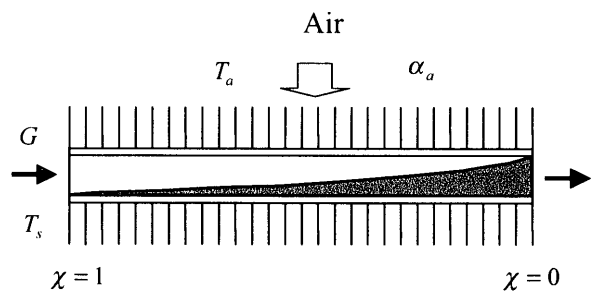

Fig.1 Schematic diagram of the air-cooled condenser

the air and refrigerant temperatures 20 and 50 ℃, respectively. Following the current design practice of manufacturers, the tube outside diameter d_o is assumed to be 7.0mm, $d = 6.5$ mm, the air-side heat transfer coefficient α_a= 135 W/m^{2}K, the outside-to-inside surface area (based on the core diameter) ratio $F_{ac} = 17.5$, the fin efficiency $\eta_f = 0.8$, and the thermal contact resistance of fins $R_f = 6\times10^{-5}$ m^{2}K/W. On the basis of the previous results [7, 9], in which the theoretical predictions of the stratified

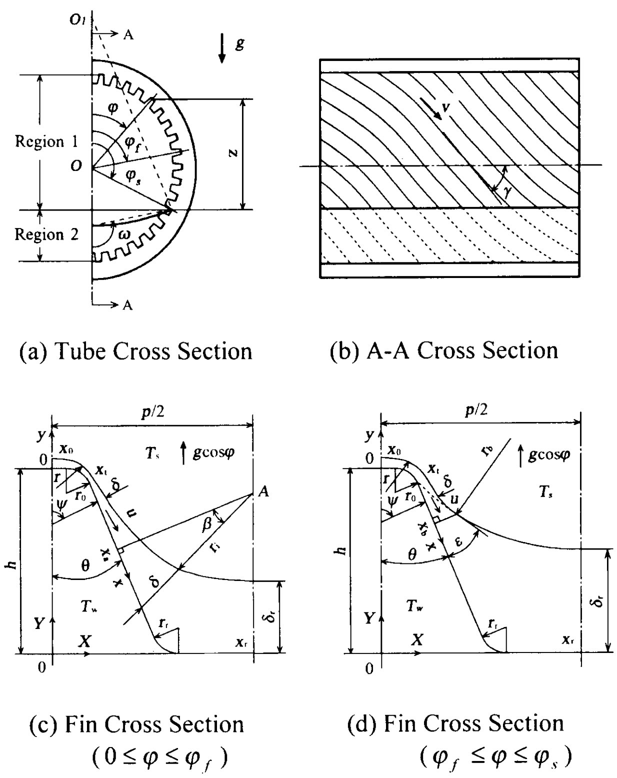

(a) Tube Cross Section (b) A-A Cross Section

(c) Fin Cross Section ($0 \le \varphi \le \varphi_f$) (d) Fin Cross Section ($\varphi_f \le \varphi \le \varphi_s$)

Fig.2 Physical model and coordinate

flow model gave a good agreement with available experimental data for R22 and R134a for the whole range of vapor quality, the stratified flow model was applied.

Figure 2 shows the physical model of stratified condensate flow in a helically grooved, horizontal microfin tube and coordinates. In Fig. 2(a), the shape of vapor-liquid interface is assumed to be a circular arc centered at O_1. The angle φ is measured from the top of the tube and φ_s denotes the angle below which the tube is filled with stratified condensate. The coordinate z is measured vertically upward from the surface of stratified condensate at $\varphi = \varphi_s$. The tube surfaces at the angular portions of $0 \le \varphi \le \varphi_s$ and $\varphi_s \le \varphi \le \pi$ are denoted as region 1 and region 2, respectively. In the region just above the level of stratified condensate, condensate is retained in the groove between adjacent fins by the capillary effect. As a result, a relatively thick condensate film is formed in the groove. The angle below which the condensate is retained in the groove is denoted as the flooding angle φ_f. Figures 2(c) and 2(d) show the condensate profiles in the fin cross-sections for regions $0 \le \varphi \le \varphi_f$ and $\varphi_f \le \varphi \le \varphi_s$, respectively. The fin profile is assumed to be a trapezoid with round corners at the fin tip and fin root. The fin height and fin pitch are h and p, respectively, and the fin half tip angle is θ. The coordinate x is measured along the tube surface from the center of fin tip and y is measured vertically outward from the tube surface. The condensate on the fin surface is drained by the combined gravity and surface tension forces toward the fin root and then it flows down the groove by gravity. Thus the condensate film thickness δ is very small near the fin tip and it is relatively thick near the fin root. The effect of vapor shear force on the condensate flow on the fin surface is assumed to be negligible.

Profile of Vapor-Liquid Interface

The profile of vapor-liquid interface is estimated by the combination of a modified Taitel and Dukler [8] model and a model of the interface configuration proposed by Brauner et al. [10]. The basic equation for the stratified flow with a curved interface is written as

$$f_v \frac{\rho_v U_v^2}{2}\frac{S_v}{A_v} - f_l \frac{\rho_l U_l^2}{2}\frac{S_l}{A_l} + f_i \frac{\rho_v U_v^2}{2}\left(\frac{S_i}{A_v} + \frac{S_i}{A_l}\right) = 0 \quad (1)$$

where f_v and f_l are the friction factors in regions 1 and 2, respectively, f_i is the interfacial friction factor, ρ_v and ρ_l are the densities of vapor and condensate, respectively, $U_v = GAx/\rho_v A_v$, $U_l = GA(1-\chi)/\rho_l A_l$, $S_v = Fd\varphi_s$, $S_l = Fd(\pi - \varphi_s)$, $S_i = d\sin\varphi_s(\pi - 2\omega)/\sin(2\omega)$,

$$A_l = \frac{d^2}{4}\left[\frac{A}{A_n}(\pi - \varphi_s) + \frac{\sin(2\varphi_s)}{2} + \sin^2\varphi_s \frac{\pi - 2\omega + \sin(4\omega)/2}{\sin^2(2\omega)}\right],$$

$A_v = \pi d^2/4 - A_l$, A is the actual cross sectional area of the tube, A_n is the nominal cross sectional area based on the fin root diameter d , F is the surface area enhance-ment as compared to a smooth tube. The expressions for f_v, f_l and f_i are given in [7].

Following Brauner et al. [10], the interface curvature is assumed to be determined by the condition that the sum of the gravitational potential and surface energy Δe is minimum, where Δe is given by

$$\Delta e = \frac{1}{8}(\rho_l - \rho_v)gd^3[\sin^3\varphi_s(\cot(2\omega) + \cot\varphi_s)\cdot \frac{\pi - 2\omega + \sin(4\omega)/2}{\sin^2(2\omega)} + \frac{2}{3}\sin^3\varphi_s^p + \frac{8}{Bo}\{\sin\varphi_s \frac{\pi - 2\omega}{\sin(2\omega)} - \sin\varphi_s^p + \cos\varsigma(\varphi_s - \varphi_s^p)\}] \quad (2)$$

where $Bo = (\rho_l - \rho_v)gd^2/\sigma$ is the Bond number, φ_s^p is the value of φ_s for a plane interface ($\omega = \pi/2$), and ς is the wettability angle. It is relevant to note here that $\varsigma = 0$ for condensation.

Profile of Thick Condensate Film

In the angular portion $\varphi_f \le \varphi \le \varphi_s$, the condensate velocity in the thick film is supposed to be very small. Thus its profile is approximated by a static meniscus that touches the fin flank (shown by a dotted line in Fig. 2(d)). Then the radius of curvature of the thick film r_b is given by

$$\frac{\sigma}{r_b} = (\rho_l - \rho_v)gz = \frac{(\rho_l - \rho_v)gd}{2}(\cos\varphi - \cos\varphi_s) \quad (3)$$

Profile of Thin Condensate Film

In the thin film region $0 \le \varphi \le \varphi_f$, δ is assumed to be sufficiently smaller than h and p. The condensate on the fin surface is drained in the x direction by the combined surface tension and gravity forces. Also, it is drained along the groove by the gravity force. The condensate flow is assumed to be laminar. Substituting the solutions of condensate velocities in the x and φ directions into the continuity equation yields

$$-\frac{(\rho_l-\rho_v)g\cos\varphi}{3\nu_l}\frac{\partial}{\partial x}\left(\sin\psi\delta^3\right)-\frac{\sigma}{3\nu_l}\frac{\partial}{\partial x}\left\{\frac{\partial}{\partial x}\left(\frac{1}{r}\right)\delta^3\right\}+\frac{2(\rho_l-\rho_v)g\sin^2\gamma}{3\nu_l d}\frac{\partial}{\partial\varphi}\left(\sin\varphi\delta^3\right)=\frac{\lambda_l(T_s-T_{w1})}{h_{fg}\delta} \quad (4)$$

where $r=r(\delta, d\delta/dx, d^2\delta/dx^2)$ is the radius of curva-ture of the condensate surface in the fin cross-section. The expression for r is given in [7]. The boundary conditions are

$$\partial\delta/\partial\varphi=0 \quad \text{at} \quad \varphi=0 \quad (5)$$

$$\partial\delta/\partial x=\partial^3\delta/\partial x^3=0 \quad \text{at} \quad x=0 \ \text{and} \ x_r \quad (6)$$

For $\varphi_f \le \varphi \le \varphi_s$, where the condensate film is consisted of a thin film region near the fin tip and a thick film region near the fin root, the boundary conditions at the connecting point between the thin film and thick film are given by

$$\partial\delta/\partial x=\tan\varepsilon, \quad r=-r_b \quad \text{at} \quad x=x_b \quad (7)$$

where ε is the angle shown in Fig. 2(d).

The solution of Eq. (4) subject to the boundary conditions (5) and (6) for $0 \le \varphi \le \varphi_f$, and (5) and (7) for $\varphi_f \le \varphi \le \varphi_s$ was obtained numerically by a finite difference scheme. The description on the numerical scheme is given in [7].

Wall Temperature and Heat Transfer Coefficients

For region 1, the average heat transfer coefficient for the fin cross section α_φ is defined on the projected area basis as

$$\alpha_\varphi=\frac{2}{p}\int_0^{x_r}\alpha_x dx=\frac{2}{p}\int_0^{x_r}\frac{\lambda_l}{\delta}dx \quad (8)$$

where $\alpha_x=\lambda_l/\delta$ is the local heat transfer coefficient. The average heat transfer coefficient for region 1, α_1, is defined on the projected area basis as

$$\alpha_1=\frac{1}{\varphi_s}\int_0^{\varphi_s}\alpha_\varphi d\varphi=\frac{2\lambda_l}{p\varphi_s}\int_0^{\varphi_s}\int_0^{x_r}\frac{1}{\delta}dxd\varphi \quad (9)$$

The heat transfer coefficient in region 2, α_2, is assumed to be uniform. The α_2 is estimated using the following empirical equation for forced convection in internally finned tubes developed by Carnavos [11]

$$\alpha_2=0.023\frac{\lambda_l}{d_l}\left(\frac{\rho_l d_l U_l}{\mu_l}\right)^{0.8}\mathrm{Pr}_l^{0.4}\left(\frac{A}{A_c}\right)^{0.1}F^{0.5}(\sec\gamma)^3 \quad (10)$$

where $A_c=\pi(d-2h)^2/4$ is the core flow area and γ is the helix angle of the groove.

The condensation temperature difference (T_s-T_{wk}) and the heat flux q_k for region k are obtained from

$$q_k=\left\{\frac{1}{\alpha_k}+\frac{d}{2\lambda_w}\ln\left(\frac{d_o}{d}\right)+R_f\frac{d}{d_o}+\frac{d}{\alpha_a\eta_f F_{ac}d_c}\right\}^{-1}(T_s-T_a)$$
$$=\alpha_k(T_s-T_{wk}) \qquad k=1,2 \quad (11)$$

where T_{wk} is the inside tube wall temperature for region k. Then the circumferential average heat transfer coefficient $\alpha_{m\varphi}$ and the average heat transfer coefficient of the condenser α_{mc} are respectively obtained from

$$\alpha_{m\varphi}=q_m/(T_s-T_{wm}) \quad (12)$$

$$\alpha_{mc}=\frac{1}{4}dGh_{fg}\Big/\int_0^l(T_s-T_{wm})dl \quad (13)$$

where

$$q_m=\{\varphi_s q_1+(\pi-\varphi_s)q_2\}/\pi \quad (14)$$

$$T_s-T_{wm}=\{\varphi_s(T_s-T_{w1})+(\pi-\varphi_s)(T_s-T_{w2})\}/\pi \quad (15)$$

T_{wm} is the circumferential average wall temperature and l is the tube length required for complete condensation.

Calculation Procedure

Numerical calculation was conducted for the range of $1-\chi=0.025\sim0.975$ with an increment of 0.05. For each $(1-\chi)$, the interface configuration was obtained from Eqs. (1) and (2). For region k (k = 1, 2), the wall temperature T_{wk} and the heat flux q_k were obtained from Eq. (11). It is relevant to note here that T_{w1} in Eq. (4) is not known a priori. Thus Eqs. (4), (9) and (11) were solved iteratively starting with an appropriate assumption of T_{w1}.

NUMERICAL RESULTS

Figures 3(a) and 3(b) show examples of the variations of T_{w1}, T_{w2}, T_{wm} and $\alpha_{m\varphi}$ with the wetness fraction $(1-\chi)$. The refrigerant mass velocity G is assumed to be 100 and 300 kg/m^{2}s, and the fin geometry parameters h, p, x_0, r_0, γ and θ are assumed to be 0.24mm, 0.4mm, 0.01mm, 0.02mm, 13° and 16°, respectively. As a result of neglecting the effect of vapor shear force on the thin condensate film, T_{w1} takes almost the same value for $G=100$ and 300 kg/m^{2}s. The condensation temperature difference in region 1, (T_s-T_{w1}), is almost constant in the region of $(1-\chi)=0\sim0.9$ and it decreases slightly with further increasing $(1-\chi)$. The condensation temperature difference in region 2, (T_s-T_{w2}), increases gradually as $(1-\chi)$ increases. The value of (T_s-T_{w2}) is much smaller for $G=300$ kg/m^{2}s than for 100 kg/m^{2}s, which is due to a higher convective heat transfer in region 2. Thus T_{wm} decreases more quickly for $G=100$ kg/m^{2}s. The temperature drop at the air-side $(T_{wm}-T_a)$ ranges from 43 to 79% of the overall temperature drop (T_s-T_a) depending on G and χ. The $\alpha_{m\varphi}$ value decreases sharply near the inlet and then it decreases gradually with increasing $(1-\chi)$. It then decreases sharply near the

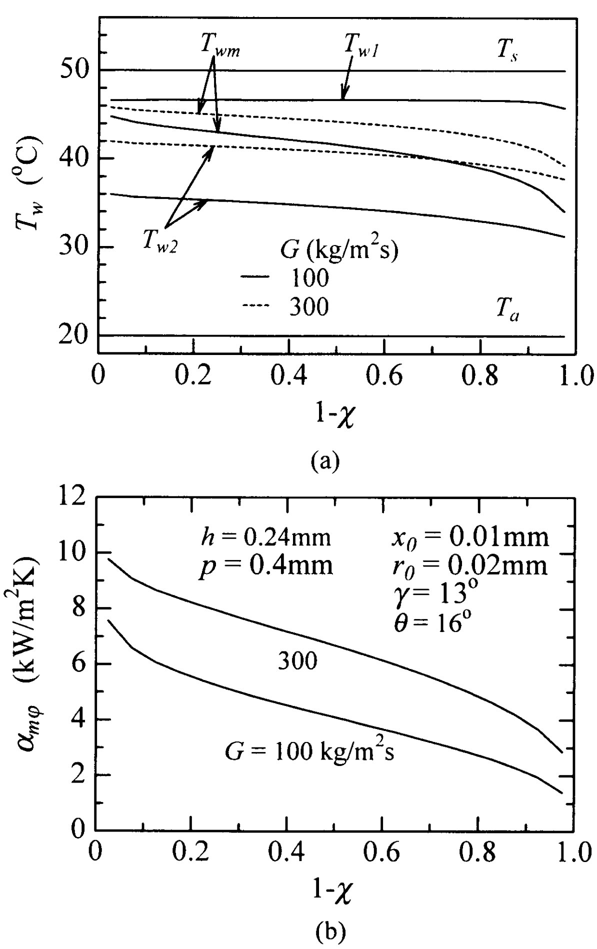

Fig.3 Variation of T_{w1}, T_{w2}, T_{wm} and $\alpha_{m\varphi}$ with 1-χ
h=0.24mm, p=0.4mm, x_0=0.01mm, r_0=0.02mm, γ=13°, θ=16°

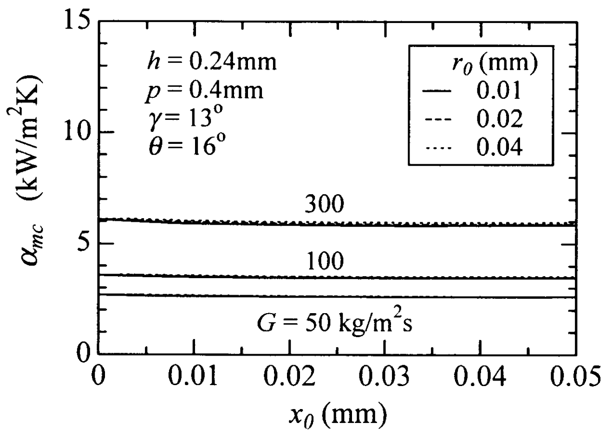

Fig.4 Variation of α_{mc} with x_0

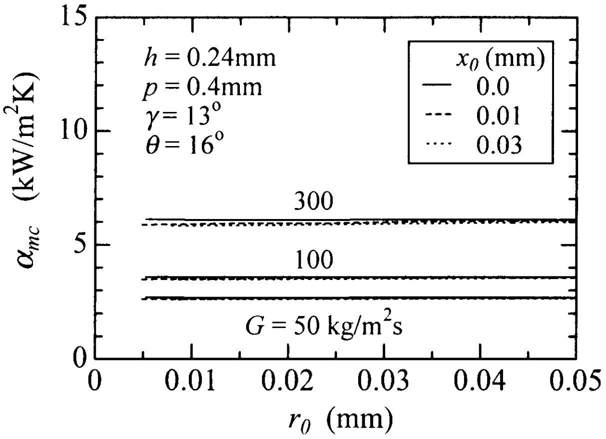

Fig.5 Variation of α_{mc} with r_0

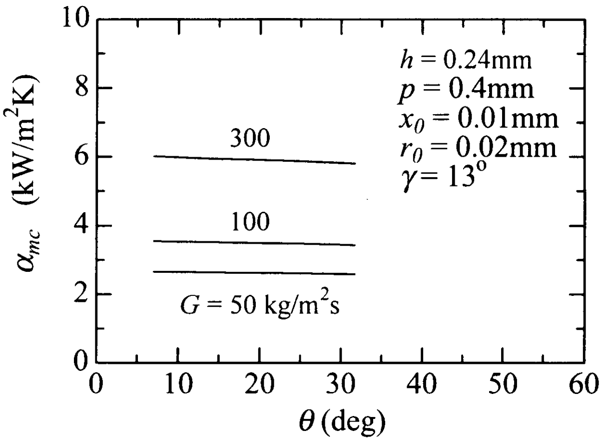

Fig.6 Variation of α_{mc} with θ

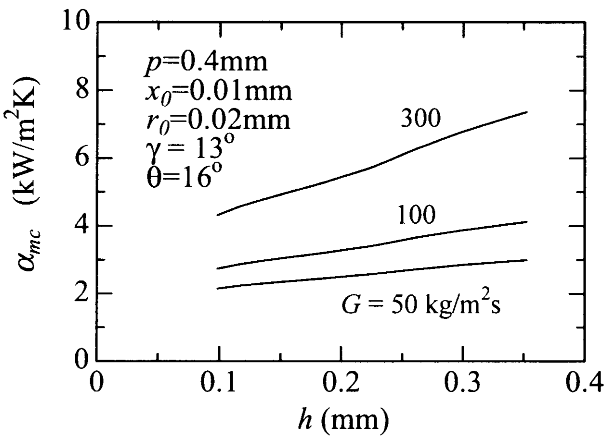

Fig.7 Variation of α_{mc} with h

outlet of the condenser.

Figure 4 shows α_{mc} plotted as a function of the length of flat portion at the fin tip x_0 with G and the radius of curvature at the corner of fin tip r_0 as parameters. The α_{mc} decreases slightly as x_0 increases and it is almost constant for $x_0 > 0.01$ mm. The α_{mc} is slightly higher for larger r_0.

Figure 5 shows α_{mc} plotted as a function of r_0 with G and x_0 as parameters. For $x_0 = 0$, α_{mc} takes a nearly constant value. For $x_0 = 0.01$ and 0.03mm, on the other hand, α_{mc} increases slightly as r_0 increases. The

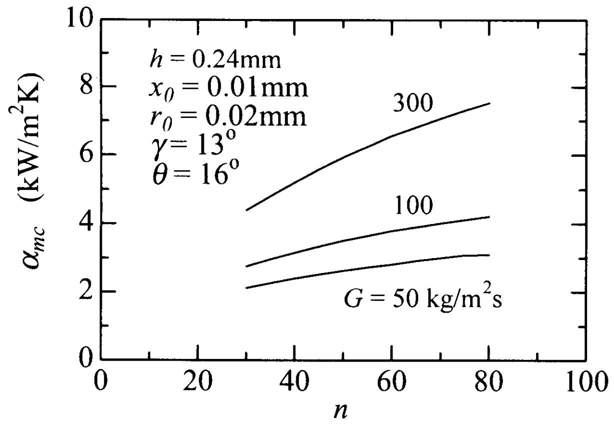

Fig.8 Variation of α_{mc} with n

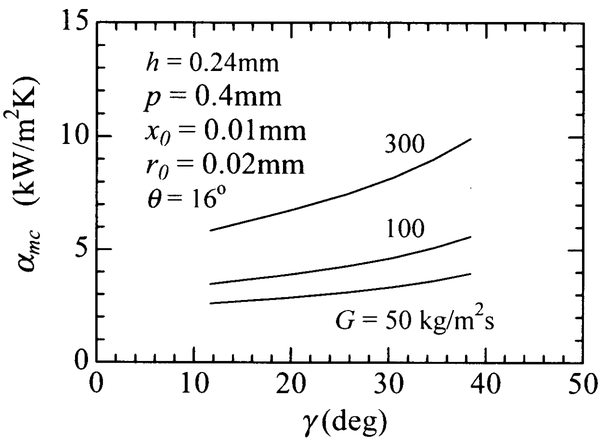

Fig.9 Variation of α_{mc} with γ

α_{mc} is slightly higher for smaller x_0. It is seen from Figs. 4 and 5 that the effects of x_0 and r_0 are rather small.

Figure 6 shows α_{mc} plotted as a function of the fin half tip angle θ with G as a parameter. The α_{mc} decreases slightly as θ increases.

Figure 7 shows α_{mc} plotted as a function of fin height h with G as a parameter. The α_{mc} increases as h increases. This is due to the increase in the effective heat transfer area near the fin tip. The effect is more significant for larger G.

Figure 8 shows α_{mc} plotted as a function of the fin number n with G as a parameter. The α_{mc} increases as n increases. The increase is more marked for smaller n and larger G. This is due to the combined effects of surface area increase and thickening of condensate film near the fin root, which is caused by the decrease in the groove width as a result of the increase in n.

Figure 9 shows α_{mc} plotted as a function of the helix angle γ with G as a parameter. The α_{mc} shows a pronounced increase as γ increases. This is due to the increase in the component of gravity along the groove and decrease in the groove length between $\varphi = 0$ and $\varphi = \varphi_s$ (see Figs. 2(a) and 2(b)), which act to augment the drainage of condensate in the groove and increase the effective heat transfer area.

It is seen from Figs. 7-9 that the effects of h, n and γ are more significant for larger G. This is due to the fact that the heat transfer coefficient in region 2, α_2, increases as G increases. This results in the increase in q_2 and decrease in $(T_s - T_{w2})$ given by Eq. (11). As a result, α_{mc} (defined by Eq. (13)) becomes more sensitive to the variation of α_1 as G increases.

It is of interest to compare the present results with previous work [12~14] reporting on the effects of fin geometry. Generally, the experimental results show that α_{mc} first increases with increasing h and n. Satoh and Nosetani [13] and Ohtani et al. [14] have reported optimum values of n that depended on d_o and γ. Ohtani et al. [14] have reported optimum values of h that depended on d_o. Satoh and Nosetani [13] have reported a decrease in α_{mc} with increasing γ, whereas Ohtani et al. [14] have reported an increase in α_{mc} with increasing γ. Since the uncertainties of the measured α_{mc} values are not described in these papers, the foregoing results are not conclusive. More accurate experimental data are required to confirm the present numerical results.

CONCLUSION

A theoretical study has been made to optimize the fin geometry of a helically-grooved, horizontal microfin tube for condensation of R410A. Numerical calculations of vapor-to-coolant heat transfer were conducted for typical operating conditions of an air-cooled condenser. The numerical results showed that the effects of the length of flat portion at the fin tip x_0, radius of round corner at the fin tip r_0 and the fin half tip angle θ are small and the effects of the fin height h, fin number n and helix angle of groove γ are of significance.

NOMENCLATURE

A	=	cross-sectional area of tube, m²
Bo	=	Bond number
d	=	diameter at fin root , m
d_l	=	equivalent diameter of liquid space, m ($=4A_l/S_i$)
d_o	=	outside diameter, m
e	=	energy, J/m
F	=	surface area enhancement as compared to a smooth tube
F_{ac}	=	outside-to-inside surface area ratio
f	=	friction factor
g	=	gravitational acceleration, m/s²
G	=	refrigerant mass velocity, kg/m²s
h	=	fin height, m
h_{fg}	=	specific enthalpy of evaporation, J/kg
l	=	tube length, m
n	=	number of fins
p	=	fin pitch, m

Pr	=	Prandtl number
q	=	heat flux, W/m^2
R_f	=	thermal contact resistance, m^2K/W
r	=	radius of curvature of condensate surface in fin cross-section, m
r_0	=	radius of curvature at corner of fin tip, m
r_b	=	radius of curvature of condensate surface in thick film region, m
r_r	=	radius of curvature at corner of fin root, m
S	=	perimeter length, m
T	=	temperature, ℃
U	=	velocity in axial direction, m/s
x, y	=	coordinates, Fig. 2
x_b	=	coordinate at connecting point between thin and thick film regions, Fig. 2, m
x_0, x_t	=	coordinates at connecting points between straight and round portions of fin, Fig. 2, m
x_r	=	mid point between adjacent fins, m
z	=	vertical height measured from condensate surface, fig. 2, m

Greek symbols

α	=	heat transfer coefficient, W/m^2K
β	=	angle, Fig. 2, deg
γ	=	helix angle of groove, deg
δ	=	condensate film thickness, m
ε	=	angle, Fig. 2, deg
ς	=	wettability angle, deg
η_f	=	fin efficiency
θ	=	fin half tip angle, deg
λ	=	thermal conductivity, W/mK
ν	=	kinematic viscosity, m^2/s
ρ	=	density, kg/m^3
σ	=	surface tension, N/m
φ	=	angle measured from tube top, deg
χ	=	mass quality
ψ	=	angle, Fig.2, deg
ω	=	angle, Fig. 2, deg

Subscripts

a	=	air side
b	=	boundary of thin and thick film regions
c	=	condenser
f	=	flooding point
i	=	liquid-vapor interface
l	=	liquid
m	=	circumferential average value
r	=	fin root, fin root mid point
s	=	saturation
v	=	vapor
w	=	wall
x	=	local value
φ	=	average value for fin cross-section
1	=	region 1
2	=	region 2

REFERENCES

1. Webb, R. L., Principles of Enhanced Heat Transfer, Chapter 14 (1994), John Wiley and Sons.
2. Newell, T. A. and Shah, R. K., Refrigerant Heat Transfer, Pressure Drop, and Void Fraction Effects in Microfin Tubes, Proceedings of 2nd International Symposium on Two-Phase Flow and Experimentation, Pisa, Italy, Vol. 3 (1999), pp. 1623-1639.
3. Cavallini, A., Doretti, L., Klammsteiner, N., Longo, G. A. and Rosetto, L., Condensation of New Refrigerants Inside Smooth and Enhanced Tubes, Proceedings of 19th International Congress of Refrigeration, Vol. IV (1995), pp. 105-114.
4. Shikazono, N., Itoh, M., Uchida, M., Fukushima, T. and Hatada, T., Predictive Equation Proposal for Condensation Heat Transfer Coefficient of Pure Refrigerants in Horizontal Microfin Tubes, Transactions of JSME, Vol. 64 (1998), pp. 196-203.
5. Yang, C. Y. and Webb, R. L., A Predictive Model for Condensation in Small Hydraulic Diameter Tubes Having Axial Microfins, ASME Journal of Heat Transfer, Vol. 119 (1997), pp. 776-782.
6. Nozu, S. and Honda, H., Condensation of Refrigerants in Horizontal, Spirally Grooved Microfin Tubes: Numerical Analysis of Heat Transfer in Annular Flow Regime, ASME Journal of Heat Transfer (2000), (to be published).
7. Honda, H., Wang, H. S. and Nozu, S., A Theoretical Model of Film Condensation in Horizontal Microfin Tubes, Proceedings of 34th National Heat Transfer Conference, Pittsburgh, Pennsylvania (2000), NHTC-12213.
8. Taitel, Y. and Dukler, A. E., A Model for Predicting Flow Regime Transitions in Horizontal and Near Horizontal Gas-Liquid Flow, AIChE Journal, Vol. 22 (1976), pp. 47-55.
9. Wang, H. S. and Honda, H., Effect of Tube Diameter on Condensation of Refrigerants in Horizontal Microfin Tubes, Proc. 37th Heat Transfer Symposium of Japan (to be published)
10. Brauner, N., Rovinsky, J. and Maron, D. M., Determination of the Interface Curvature in Stratified Two-Phase Systems by Energy Considerations, Inter-national Journal of Multiphase Flow, Vol.22 (1996), pp.1167-1185.
11. Carnavos, T. C., Heat Transfer Performance of Internally Finned Tubes in Turbulent Flow, Heat Transfer Engineering, Vol. 4 (1980), pp. 32-37.
12. Hori, M. and Shinohara, Y., J. Japan Copper and Brass Research Assoc., Vol. 29 (1990), pp.65-70.
13. Satoh, Y. and Nosetani, K., J. Japan Copper and Brass Research Assoc., Vol.29 (1990), pp.233-239.
14. Ohtani, T., Tsuchita, T., Yasuda, K. and Hori, N., Hitachi Densen, Vol. 13, (1994), pp.115-120.